Versão online: http://www.lneg.pt/iedt/unidades/16/paginas/26/30/125

Comunicações Geológicas

Comunicações Geológicas (2012) 99, 2, 101-105
ISSN: 0873-948X; **e-ISSN:** 1647-581X

ID-TIMS U-Pb geochronology and some notes on the geodynamic and geochemical evolution of the high grade rocks of central Ribeira Fold Belt (SE Brazil)

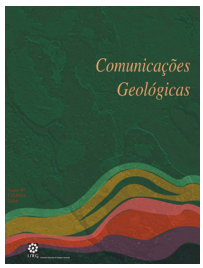

Geocronologia ID-TIMS U-Pb e algumas ideias sobre a evolução geodinâmica e geoquímica das rochas de alto grau da zona central da Faixa Ribeira (SE do Brasil)

T.M. Bento dos Santos[1, 2*], C.C.G. Tassinari[3], J.M. Munhá[2], P.E. Fonseca[2]

Recebido em 19/03/2012 / Aceite em 16/05/2012
Disponível *online* em Maio de 2012 / Publicado em Dezembro de 2012
© 2012 LNEG – Laboratório Nacional de Geologia e Energia IP

Artigo original
Original article

Abstract: The studied sector comprises high grade metamorphic rocks formed during the Neoproterozoic – Ordovician evolution of central Ribeira Fold Belt (SE Brazil). The new ID-TIMS U-Pb geochronological results for a charnockite and a diatexite of the studied area suggest that metamorphic peak conditions occurred at ~570 Ma. These results further support the idea that both extensive production of granitoid melts (diatexites) and charnockite/granulite formation in the area was simultaneous and that the recently suggested genetic relation between these rock types is consistent.

Keywords: Western Gondwana, Ribeira Fold Belt, geochronology, granulite, diatexite.

Resumo: O sector estudado compreende rochas metamórficas de alto grau formadas durante a evolução Neoproterozóica – Ordovícica da zona central da Faixa Ribeira (SE do Brasil). Os novos resultados geocronológicos U-Pb (ID-TIMS) obtidos para um charnockito e um diatexito da área estudada sugerem que as condições de pico metamórfico ocorreram há ~570 Ma. Estes resultados reforçam a ideia de que tanto a produção generalizada de líquidos granitóides (diatexitos) como a formação de charnockitos/granulitos na área foi simultânea e que a relação de parentesco recentemente sugerida para estas rochas é consistente.

Palavras-chave: Gondwana Ocidental, Faixa Ribeira, geocronologia, granulito, diatexito.

[1] LNEG – Laboratório Nacional de Energia e Geologia, Estrada da Portela – Zambujal – Alfragide, Apartado 7586, 2610-999 Amadora, Portugal.
[2] Centro de Geologia, Universidade de Lisboa, Edifício C6, 3º, Campo Grande, 1749-016 Lisboa, Portugal.
[3] Instituto de Geociências, Universidade de São Paulo, Rua do Lago, 562 – Butantã, CEP: 05508-080, São Paulo, Brazil.
* Corresponding author /Autor correspondente: telmo.santos@lneg.pt

1. Introduction

The São Fidelis region is part of the central segment of Ribeira Fold Belt (RFB), a mobile belt formed during the Pan-African Orogeny (Cordani, 1971). The RFB has been mainly studied for its connection to the West Congo Belt in Africa and the Neoproterozoic assemblage of Western Gondwana due to the collision between the São Francisco and Congo Cratons (e.g.: Cordani *et al.*, 1973).

Although geochronological results have recently been provided by several authors working on the central RFB (Heilbron & Machado, 2003; Schmitt *et al.*, 2004; 2008; Bento dos Santos *et al.*, 2010), this work presents new ID-TIMS U-Pb geochronological data from the São Fidelis region granulites (*s.l.*) with the purpose of further describing the timing and features of the peak of metamorphism, high grade partial melting (migmatization) and granulite formation in the area. The obtained results allow a better understanding of the lithological and geochemical evolution of the studied rocks, whereas the progressive compilation of isotopic data in the area provides further constraints on the geodynamic evolution of the RFB within the frame of the amalgamation of Western Gondwana.

2. Geological Setting and Field Observations

2.1. The Central Ribeira Fold Belt

The studied sector is located in the central-north segment of the RFB (Cordani, 1971), northern Rio de Janeiro State, SE Brazil (Fig. 1). The RFB extends along the SE Brazilian coast and is an elongated NE-SW trending (south and central sectors) and NNE-SSW trending (northern sector) belt that can be divided in four major lithologic associations: a) reworked Archean to Paleoproterozoic basement rocks composed of metavolcanic-sedimentary sequences, granodioritic orthogneisses and intermediate granulites; b) a deformed meta-sedimentary sequence composed of pelitic schists and high grade migmatitic paragneisses with quartzite, calc-silicate and amphibolite intercalations; c) molasic sedimentary basins; and d) widespread granitoid intrusive bodies with different tectonic settings, from pre- to post-collision stages of the Pan-African orogenic system (Trouw et. al., 2000).

The central RFB is a complex orogenic zone and is divided in four tectonic/lithologic/geochronological domains, separated by deep dextral shears, that include, from NW to SE: a) the Occidental Domain, mainly a pre-1.8 Ga passive margin sequence of basement rocks (the reworked margin of the São Francisco Craton); b) the Paraíba do Sul klippe, composed of amphibolites and amphibolite facies orthogneisses and meta-sediments; c) the Oriental Domain, where most of the the studied area is located, comprising high grade meta-sedimentary sequences, granulites and granitoids. The granulites are typically massive metamorphic charnockites and

variable sized patches and veins of incipient metamorphic charnockites associated with the meta-sedimentary sequences and orthogneisses (Bento dos Santos *et al.*, 2011a; Tassinari *et al.*, 2008); and d) the Cabo Frio Terrane (Schmitt *et al.*, 2008), an inferred allochthonous terrane belonging to the Congo Craton (Heilbron & Machado, 2003; Valladares *et al.*, 2008).

2.2. The São Fidelis region

The São Fidelis region (Fig. 1b) underwent complex polyphase deformation during the Pan-African Orogeny (Fonseca *et al.*, 2008). The earliest deformation (D_1) in the area corresponds to high angle (and high temperature) thrusts simultaneous with intense granulite facies metamorphism that produced the migmatites and granulites in the area. The São Fidelis region is located SE of a very important crustal-scale megashear, the Além Paraíba – Santo António de Pádua Shear (APPS) (Fig. 1b). This megashear vigorously deformed the rocks of the São Fidelis region imposing a NE to ENE trending D_2 transpressive shear deformation associated with long-term HT metamorphism (Bento dos Santos *et al.*, 2007; Fonseca *et al.*, 2008) that almost completely erased the D_1 strain markers. Late ductile/brittle D_3 event reactivated the D_2 conjugate faults and is associated with the intrusion of late granitoid and pegmatoid bodies (Fonseca *et al.*, 2008; Bento dos Santos *et al.*, 2009).

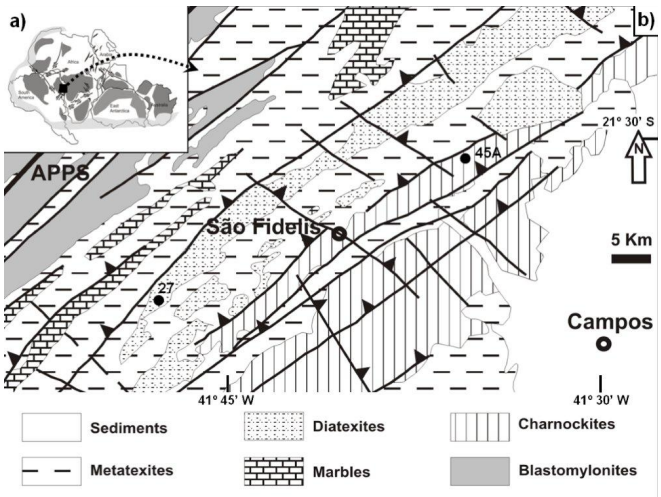

Fig.1. Geological setting of the São Fidelis region (modified from Bento dos Santos *et al.*, 2010; Bento dos Santos *et al.*, 2011a): a) Central Ribeira Fold Belt (square) in the Western Gondwana amalgamation context (modified from Piper, 2000). Box locates studied area; b) Simplified geological map of the São Fidelis region showing the main lithologic units and structures present, as well as the location of the studied samples. APPS: Além Paraíba – Santo António de Pádua Shear (modified from Bento dos Santos *et al.*, 2010).

Fig.1. Enquadramento geológico da região de São Fidelis (modificado de Bento dos Santos *et al.*, 2010; Bento dos Santos et al, 2011a): a) Faixa Ribeira central (quadrado) no contexto da amalgamação do Gondwana Ocidental (modificado de Piper, 2000). A caixa localiza a área em estudo; b) Mapa geológico simplificado da região de São Fidelis mostrando as principais unidades litológicas e estruturas presentes, bem como a localização das amostras estudadas. APPS: Cisalhamento Além Paraíba – Pádua (modificado de Bento dos Santos *et al.*, 2010).

Bento dos Santos (2008) presented an extensive geothermobarometric study of the São Fidelis region. This author obtained a T = 661 – 896 ºC and P = 7.0 – 8.9 kbar range for the metamorphic peak conditions of charnockites, metatexites and diatexites. The São Fidelis region must have achieved minimum metamorphic peak conditions of T ~ 750 ºC and P ~ 8.0 kbar, whereas the lower T and P estimates are mainly due to chemical reequilibration during retrogression (Bento dos Santos, 2008).

3. Sample Description

Extensive petrographic and mineral chemistry descriptions of the rocks of the São Fidelis region are accessible elsewhere (Bento dos Santos, 2008; Bento dos Santos *et al.*, 2011b). The São Fidelis region comprises: a) migmatitic paragneisses (metatexites) (Migmatite terminology as in Wimmenauer & Brynhi, 2007); b) diatexites (Fig. 2a-b); c) granulites (massive and incipient-type charnockites) that crop out as elongated NE-SW trending massifs (Fig. 3a-c) associated with their granitic to granodioritic orthogneiss precursors (Bento dos Santos *et al.*, 2011a) and aplites. Migmatite charnockitization is sometimes visible (Bento dos Santos *et al.*, 2011a).

Geochronological results were obtained for a diatexite (sample 27), collected 22 km SW of São Fidelis and a charnockite (sample 45A), collected 20 km NE of São Fidelis (see Fig. 1 for sample location).

Diatexites commonly comprise large elongated or rounded, undeformed and homogeneous garnet granitic to migmatitic batholiths, derived by an advanced stage of anatexis. Diatexites show a medium grain sized Pl + Qz + Kfs + Bt + Grt ± Amp (Mineral abbreviations according to Whitney & Evans, 2010) assemblage (Fig. 2c-f). The isotropic texture is frequently dominated by plagioclase and biotite, imposing a granolepidoblastic texture to the rock or in some cases, granonematoblastic, when amphibole is dominant. Garnet is commonly surrounded by symplectitic biotite and/or amphibole + quartz (Fig. 2f). No oxide minerals are present in these rocks.

Charnockites are characterized as having a massive, undeformed and isotropic texture. They are composed of a medium to coarse sized granoblastic texture with Pl + Qz + Kfs ± Grt ± Opx (Fig. 3d-f). Biotite, ilmenite and magnetite are only present as matrix minerals. Biotite and quartz symplectites are common around garnet and pyroxene rims.

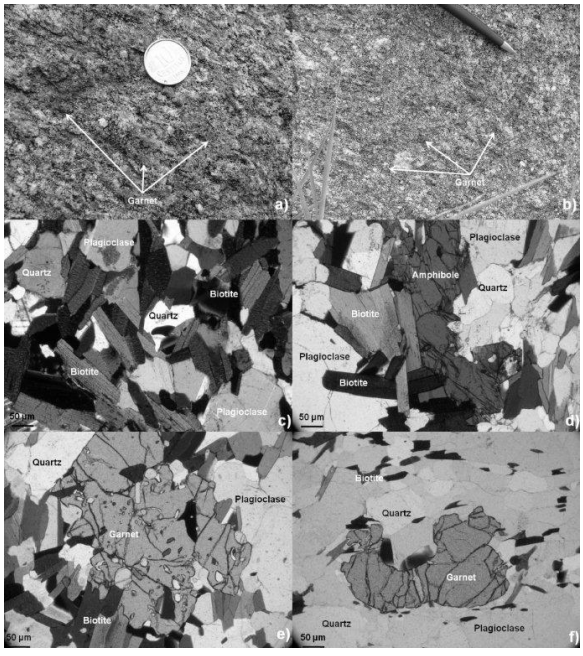

Fig. 2. a-b) Field examples of the studied diatexites (with garnet) showing an undeformed and homogeneous look; c-d) Photomicrographs of isotropic, undeformed diatexite with biotite and amphibole; e-f) Photomicrographs of diatexite with garnet.

Fig. 2. a-b) Exemplos de amostras mesoscópicas dos diatexitos estudados (com granada) evidenciando um aspecto não deformado e homogéneo; c-d) Imagens de microscópio dos diatexitos isotrópicos e não deformados com biotite e anfíbola; e-f) Imagens de microscópio de diatexito com granada.

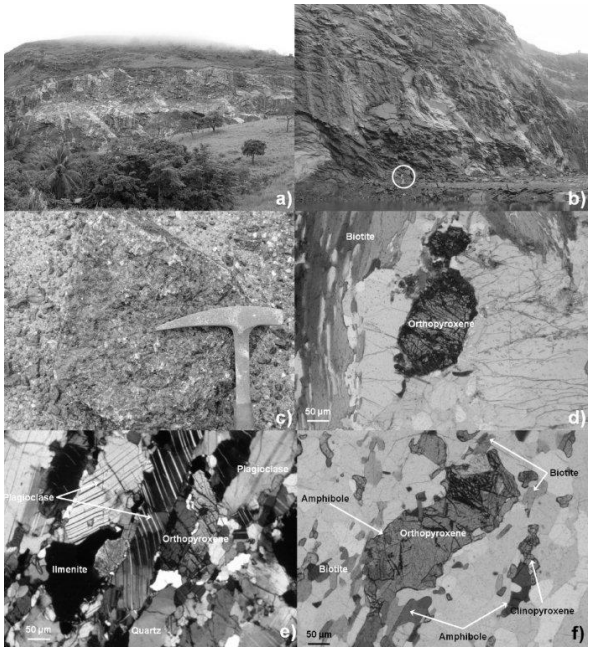

Fig. 3. a-c) Field examples of the studied massive charnockites. In b) circle evidences a person for scale purposes; d) Photomicrograph of an undeformed charnockite showing an orthopyroxene megablast surrounded by late biotite; e) Photomicrograph of a deformed charnockite; f) Photomicrograph of a charnockite showing an amphibole inclusion inside an orthopyroxene megablast.

Fig. 3. a-c) Exemplos de amostras mesoscópicas dos charnockitos estudados. Em b) um círculo realça uma pessoa para efeitos de escala; d) Imagem de microscópio de um charnockito não deformado, evidenciando um megablasto de ortopiroxena rodeado por biotite tardia; e) Imagem de microscópio de um charnockito deformado; f) Imagem de microscópio de um charnockito, evidenciando uma inclusão de anfíbola no interior de um megablasto de ortopiroxena.

4. Analytical Methods

Samples were prepared at the Instituto de Geociências da Universidade de São Paulo (IGc-USP) and at the Departamento de Geologia da Universidade de Lisboa (DG-FCUL).

The ID-TIMS U-Pb geochronological results were obtained in the Centro de Pesquisa Geocronológica (CPGeo) of the IGc-USP. Standard analytical procedures were used for the isotopic analyses as described by Tassinari *et al.* (2003) and Sato *et al.* (1995). Mineral separation and concentration follows routine procedures of the CPGeo Separation Lab, as described by Basei *et al.* (1995). U and Pb were separated by isotopic dilution techniques according with the procedures developed by Krogh (1973) and Parrish (1987). U and Pb were measured on a multi-collector Finnigan MAT262 mass spectrometer. Pb measurements were corrected using the NBS SRM-982 Pb equal atom standard and the NBS SRM-983 Pb radiogenic standard. U fractionation was monitored with the NBS SRM U-500 standard. Pb/U uncertainties are 0.5 %. The Pb blank levels were 70 pg during the period of analysis. Ages were determined using the recommended Steiger & Jaeger (1977) decay rates. Age calculations were obtained using the Ludwig (1998) ISOPLOT/Ex software. The obtained U-Pb ages are the weighted average of the obtained zircon $^{206}Pb/^{238}U$ ages or the linear regression considering Pb loss.

5. ID-TIMS U-Pb Geochronology

Zircon petrographic descriptions and geochronological results (with a 2σ error) are presented below. Obtained isotopic data can be found in Table 1.

Table 1. ID-TIMS U-Pb results in zircon concentrates obtained at the Centro de Pesquisa Geocronológica (CPGeo) of the Instituto de Geociências da Universidade de São Paulo (IGc-USP) for samples 45A and 27. Due to space constraints, isotopic notation is simplified (e.g.: 206/238 is $^{206}Pb/^{238}U$).

Tabela 1. Resultados U-Pb em ID-TIMS nos concentrados de zircão obtidos no Centro de Pesquisa Geocronológica (CPGeo) do Instituto de Geociências da Universidade de São Paulo (IGc-USP) para as amostras 45A e 27. Devido a problemas de espaço, as notações isotópicas encontram-se simplificadas (por exemplo: 206/238 significa $^{206}Pb/^{238}U$).

Fraction	Sample	Mineral	Rock	Weight (mg)	207/235	Error (%)	206/238	Error (%)	COEF.	238/206	Error (%)
3114				0.03493	0.758387	0.51	0.092043	0.49	0.958247	10.864545	0.49
3115				0.03427	0.938820	0.70	0.100899	0.56	0.796330	9.910901	0.56
3116	45A	Zircon	Charnockite	0.03427	0.772218	0.59	0.094066	0.54	0.915330	10.630822	0.54
3118				0.02297	0.757293	0.63	0.092915	0.55	0.871360	10.762513	0.55
3148				0.02857	0.755797	0.51	0.092730	0.48	0.944756	10.783997	0.48
3149				0.03252	0.742124	0.53	0.091445	0.48	0.905291	10.935487	0.48
Fraction	**Sample**	**Mineral**	**Rock**	**207/206**	**Error (%)**	**206/204**	**Pb (ppm)**	**U (ppm)**	**Age 206/238 (Ma)**	**Age 207/235 (Ma)**	**Age 207/206 (Ma)**
3114				0.059511	0.15	4022.0	45.190	462.760	569	573	585
3115				0.067483	0.42	3025.2	23.627	224.180	619	672	852
3116	45A	Zircon	Charnockite	0.059540	0.24	1566.4	25.253	255.470	579	581	586
3118				0.059112	0.31	1484.5	28.754	285.020	572	572	571
3148				0.059113	0.17	719.8	28.727	277.410	572	572	571
3149				0.058883	0.22	1435.6	34.400	345.800	564	564	562
Fraction	**Sample**	**Mineral**	**Rock**	**Weight (mg)**	**207/235**	**Error (%)**	**206/238**	**Error (%)**	**COEF.**	**238/206**	**Error (%)**
3109				0.03294	0.741631	0.48	0.090915	0.47	0.987693	10.999285	0.47
3110				0.02602	0.736056	0.48	0.090196	0.47	0.986618	11.086917	0.47
3111				0.03572	0.720782	0.50	0.088525	0.49	0.970942	11.296193	0.49
3112	27	Zircon	Diatexite	0.03052	0.729622	0.52	0.089377	0.51	0.977300	11.188598	0.51
3113				0.03204	0.781968	0.48	0.093499	0.48	0.983176	10.695256	0.48
3146				0.03052	0.732498	0.50	0.090074	0.48	0.977777	11.102020	0.48
3147				0.02726	0.717394	0.90	0.088649	0.83	0.933145	11.280430	0.83
Fraction	**Sample**	**Mineral**	**Rock**	**207/206**	**Error (%)**	**206/204**	**Pb (ppm)**	**U (ppm)**	**Age 206/238 (Ma)**	**Age 207/235 (Ma)**	**Age 207/206 (Ma)**
3109				0.059163	0.07	5774.4	57.863	629.540	560	563	573
3110				0.059186	0.08	9808.9	84.518	939.580	556	560	573
3111				0.059052	0.12	5077.1	58.825	661.080	546	551	569
3112	27	Zircon	Diatexite	0.059207	0.11	1971.6	49.342	535.710	551	556	574
3113				0.060657	0.09	6139.7	59.020	621.680	576	586	627
3146				0.058980	0.10	5691.0	54.023	585.260	556	558	566
3147				0.058693	0.32	2301.1	69.320	755.780	548	549	556

5.1. Charnockite 45A

Charnockite 45A has transparent and colourless zircons and displays two generic populations (3:1 to 6:1 elongated tabular zircons and 1.5:1 to 2:1 oval zircons – Fig. 4) ranging from 50 to 200 µm wide. They are mostly prismatic with rounded tips and show some fracturing and few inclusions. Six zircon fractions of both populations, weighting 25 to 35 µg, were dated (62 zircons) by the ID-TIMS method. The $^{207}Pb/^{206}Pb$ results range from 0.059 to 0.067. This large range is mostly due to fraction 3115 that shows a $^{207}Pb/^{206}Pb$ much higher than the others ($^{207}Pb/^{206}Pb$ = 0.0589 – 0.0595), a $^{238}U/^{206}Pb$ (9.91) very contrasting compared with the other samples ($^{238}U/^{206}Pb$ = 10.63 to 10.93) and a significantly older $^{238}U/^{206}Pb$ age (615 ± 3 Ma) when compared with the rest of the fractions (564 ± 3 to 580 ± 3 Ma). No correlation between the morphology of the fractions and the isotopic results was detected. Therefore, fractions 3114, 3116, 3118, 3148 and 3149 were used to determine the mean $^{238}U/^{206}Pb$ age (570.5 ± 7.1 Ma) (Fig. 4). Fraction 3115 age result, although discordant (619 ± 4 Ma), agrees well with the collision period in the studied area (according to Cunningham *et al.*, 1998; Janasi *et al.*, 2001; Heilbron & Machado, 2003; Silva *et al.*, 2005).

5.2. Diatexite 27

Diatexite 27 has transparent and colourless to brownish zircons and displays two common populations (5:1 to 8:1 elongated thin zircons and 2:1 to 3:1 oval zircons – Fig. 5), from 50 to 300 µm long. They are mostly prismatic with rounded tips and show limited fractures and inclusions. Seven zircon fractions of both populations, weighting 26 to 36 µg, were dated (77 zircons) by the ID-TIMS method. The $^{207}Pb/^{206}Pb$ results range from 0.0587 to 0.0607 with the highest result belonging to the discordant and very contrasting fraction 3113. This fraction also shows a lower $^{238}U/^{206}Pb$ (10.70) than the other fractions (11.0 – 11.30) and an older $^{238}U/^{206}Pb$ age of 575.3 ± 5.3 Ma in comparison with the other fractions (547.4 ± 8.7 to 561 ± 5 Ma). However, fractions 3111 and 3146 display significant discordance, suggesting Pb loss and, therefore, were not used for age calculations.

Remaining fractions (3109, 3110, 3112 and 3147) were used and provide a mean $^{238}U/^{206}Pb$ age of 555.5 ± 8.3 Ma (Fig. 5). However, observation of Fig. 5 stongly suggests that Pb loss was important for fractions 3109, 3110, 3147, 3112 and 3111. Considering a possible Pb loss for these fractions, linear regression provides a concordia age of 569.5 ± 9.0 Ma age for this sample (Fig. 5).

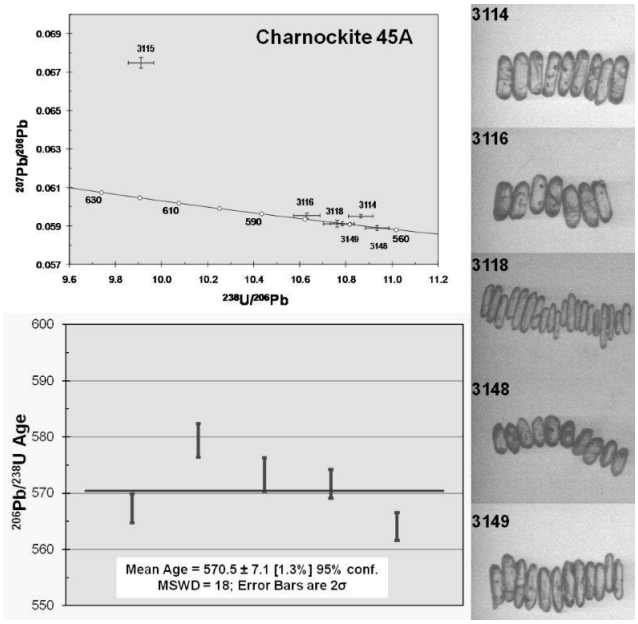

Fig. 4. Zircon petrography, Tera-Wasserburg diagram and $^{238}U/^{206}Pb$ age results for charnockite 45A. Fractions used for mean $^{238}U/^{206}Pb$ age are shown.

Fig. 4. Petrografia dos zircões, diagrama Tera-Wasserburg e resultados das idades $^{238}U/^{206}Pb$ para o charnockito 45A. As fracções usadas para a média das idades $^{238}U/^{206}Pb$ encontram-se realçadas.

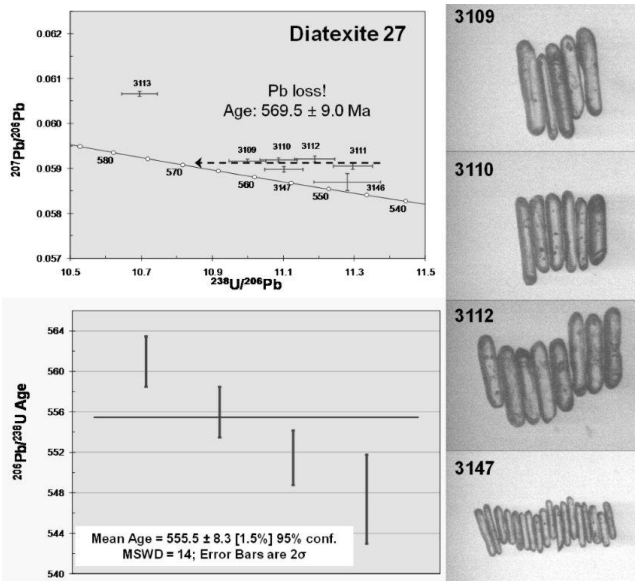

Fig. 5. Zircon petrography, Tera-Wasserburg diagram and $^{238}U/^{206}Pb$ age results for diatexite 27. Fractions used for mean $^{238}U/^{206}Pb$ age are shown. Linear regression (considering Pb loss) for samples 3109, 3110, 3111, 3112 and 3147 provides a concordia age of 569.5 ± 9.0 Ma.

Fig. 5. Petrografia dos zircões, diagrama Tera-Wasserburg e resultados das idades $^{238}U/^{206}Pb$ para o diatexito 27. As fracções usadas para a média das idades $^{238}U/^{206}Pb$ encontram-se realçadas. Regressão linear (considerando perda de Pb) para as amostras 3109, 3110, 3111, 3112 e 3147 fornece uma idade concórdia de 569.5 ± 9.0 Ma.

5. Conclusions

The ID-TIMS results for charnockite 45A and diatexite 27 provided $^{238}U/^{206}Pb$ ages from 570.5 ± 7.1 to 569.5 ± 9.0 Ma, identical ages considering the analytical error. These results are comparable with previous results obtained on high-grade rocks of central RFB that range from 572 ± 13 to 566 ± 12 Ma (Bento dos Santos *et al.*, 2010) and 562 Ma ± 11 Ma (Schmitt *et al.*, 2004). Age clustering around 570 Ma indicates that the generation of charnockites and diatexites was approximately simultaneous, as predicted by recent geochemical studies developed by Bento dos Santos *et al.* (2011a). These authors suggest a genetic link between the meta-sedimentary rocks (metatexites and diatexites) and the charnockites in the area. The obtained results contradict previously assumed age gap between magmatic age and the thermal paroxysm that Dias Neto (2001) suggested to be ~580 Ma and ~570 Ma, respectively. Regarding the geodynamic evolution of central RFB, the present results indicate that after the collision of the São Francisco and the Congo cratons at 630 – 610 Ma (Cunningham *et al.*, 1998; Janasi *et al.*, 2001; Heilbron & Machado, 2003; Silva *et al.*, 2005), D_1 thrust deformation phase and metamorphic peak with abundant partial melting of the crust and granulite generation occurred at ~ 570 Ma. This is also the most probable age for the onset of the thermal anomaly described by Bento dos Santos *et al.* (2010). This period of elevated geothermal gradients may have lasted from ~570 Ma to 510 – 480 Ma (beginning of the D_4 deformation events; Bento dos Santos *et al.*, 2010) and probably reflected upwelling of asthenospheric mantle and magma underplating along the main axis of central RFB as the result of post-collision thermal erosion and lithosphere thinning (Bento dos Santos *et al.*, 2007).

Acknowledgements

FAPESP, POCA-PETROLOG (CEGUL, UI: 263; POCTI/FEDER), GEODYN (POCTI – ISFL – 5 – 32) and a PhD scholarship from FCT (SFRH/BD/17014/2004) co-financed by FEDER provided support for field and analytical work. A post-doc scholarship from LNEG supported the corresponding author during the preparation of this work.

References

Basei, M., Siga Jr., O., Sato, K., Sproesser, W., 1995. A Metodologia U-Pb na Universidade de São Paulo. Princípios metodológicos, aplicações e resultados obtidos. *Anais da Academia Brasileira de Ciências*, **67**, 2, 221-237.

Bento dos Santos, T., 2008. Petrologia e termocronologia de granulitos no sector central da Faixa Ribeira (Região de São Fidelis, Rio de Janeiro, Brasil). *Unpublished Ph.D. thesis*, University of Lisbon, Lisbon, 388.

Bento dos Santos, T., Fonseca, P., Munhá, J., Tassinari, C., Dias Neto, C., 2009. Geodynamic evolution of the São Fidelis – Santo Antônio de Pádua sector, Ribeira Fold Belt, SE Brazil. *Comunicações Geológicas*, **96**, 101-122.

Bento dos Santos, T., Munhá, J., Tassinari, C., Fonseca, P., 2011a. The link between partial melting, granitization and granulite development in central Ribeira Fold Belt, SE Brazil: new evidence from elemental and Sr-Nd isotopic geochemistry. *Journal of South American Earth Sciences*, **31**, 2-3, 262-278.

Bento dos Santos, T., Munhá, J., Tassinari, C., Fonseca, P., Dias Neto, C., 2007. Thermochronological evidence for long-term elevated geothermal gradients in Ribeira Belt, SE Brazil. *Geochimica et Cosmochimica Acta*, **71**, 15, 1, A79.

Bento dos Santos, T., Munhá, J., Tassinari, C., Fonseca, P., Dias Neto, C., 2010. Thermochronology of central Ribeira Fold Belt, SE Brazil: Petrological and geochronological evidence for high-temperature maintenance during Western Gondwana amalgamation. *Precambrian Research*, **180**, 3-4, 285-298.

Bento dos Santos, T., Munhá, J., Tassinari, C., Noronha, F., Guedes, A., Fonseca, P., Dias Neto, C., Dória, A., 2011b. P-T-Fluid evolution and graphite deposition during retrograde metamorphism in Ribeira Fold Belt, SE Brazil: oxygen fugacity, fluid inclusions and C-O-H isotopic evidence. *Journal of South American Earth Sciences*, **31**, 1, 93-109.

Cordani, U., 1971. Síntese da geocronologia Pré-Cambriana da região costeira atlântica meridional da América do Sul. *25th Congresso Brasileiro de Geologia*, São Paulo, 179-180.

Cordani, U., Delhal, J., Ledent, D., 1973. Orogenéses superposées dans le Précambrien du Brésil sud-oriental (États de Rio de Janeiro et de Minas Gerais). *Revista Brasileira de Geociências*, **3**, 1-22.

Cunningham, D., Alkmin, F., Marshak, S., 1998. A structural transect across the coastal mobile belt in the Brazilian Highlands (latitude 20ºS): the roots of a Precambrian transpressional orogen. *Precambrian Research*, **92**, 251-275.

Dias Neto, C. M., 2001. Evolução tectono-termal do complexo Costeiro, faixa de dobramentos Ribeira em São Paulo. *Unpublished PhD Thesis*, University of São Paulo, São Paulo, 160.

Fonseca, P., Bento dos Santos, T., Munhá, J., Tassinari, C., Dias Neto, C., 2008. Thermochronological and structural analysis of the geodynamic evolution of Ribeira Belt, SE Brazil. *Geochimica et Cosmochimica Acta*, **72**, 12, 1, A276.

Heilbron M., Machado, N., 2003. Timing of Terrane Accretion in the Neoproterozoic-Eopaleozoic Ribeira Orogen SE Brazil. Precambrian Research, 125, 87-112.

Janasi, V., Leite, R., Van Schmus, W., 2001. U-Pb chronostratigraphy of the granitic magmatism in the Agudos Grandes Batholith (West of São Paulo, Brazil) – implications for the evolution of the Ribeira Belt. *Journal of South American Earth Sciences*, **14**, 363-376.

Krogh, T., 1973. A low contamination method for hydrothermal decomposition of zircon and extraction of U and Pb for isotopic age determinations. *Geochimica et Cosmochimica Acta*, **37**, 485-494.

Ludwig, K., 1998. *Isoplot/Ex. Berkeley Geochronological Centre Special Publication*, **1**.

Parrish, R., 1987. An improved micro-capsule for zircon dissolution in U-Pb geochronology. *Chemical Geology*, **66**, 99-102.

Piper, J., 2000. The Neoproterozoic Supercontinent: Rodinia or Paleopangea? *Earth and Planetary Science Letters*, **176**, 131-146.

Sato, K., Tassinari, C., Kawashita, K., Petronillo, L., 1995. O método geocronológico Sm-Nd no IGc/USP e suas aplicações. *Anais da Academia Brasileira de Ciências*, **67**, 3, 315-336.

Schmitt, R., Trouw, R., Medeiros, S., Dantas, E., 2008. Age and geotectonic setting of Late Neoproterozoic juvenile mafic gneisses and associated paragneisses from the Ribeira Belt (SE Brazil) based on geochemistry and Sm – Nd data – Implications on Gondwana assembly. *Gondwana Research*, **13**, 4, 502-515.

Schmitt, R., Trouw, R., Schmus, W., Pimentel, M., 2004. Late amalgamation in the central part of West Gondwana: new geochronological data and the characterization of a Cambrian collision orogeny in the Ribeira Belt (SE Brazil). *Precambrian Research*, **133**, 29-61.

Silva, L., McNaughton, N., Armstrong, R., Hartmann, L., Fletcher, I., 2005. The Neoproterozoic Mantiqueira Province and its African connections: a zircon-based U-Pb geochronological subdivision for the Brasiliano/Pan-African systems of orogens. *Precambrian Research*, **136**, 203-240.

Steiger, R., Jaeger, E., 1977. Subcommission on geochronology: convention on the use of decay constants in geochronology and cosmochronology. *Earth and Planetary Science Letters*, **36**, 359-362.

Tassinari, C., Bento dos Santos, T., Munhá, J., Fonseca, P., 2008. Whole-rock geochemistry and Sr-Nd isotopic evidence for sources and processes of granulite formation in Ribeira Belt, Brazil. *Geochimica et Cosmochimica Acta*, **72**, 12, 1, A936.

Tassinari, C., Mellito, K., Babinski, M., 2003. Age and origin of the Cu (Au-Mo-Ag) Salobo 3a ore deposit, Carajás Mineral Province, Amazonian Craton, northern Brazil. *Episodes*, **26**, 1, 2-9.

Trouw, R., Heilbron, M., Ribeiro, A., Paciullo, F., Valeriano, C., Almeida, J., Tupinambá, M., Andreis, R., 2000. The central segment of the Ribeira Belt. In: Cordani, U.G., Milani, E.J., Thomaz-Filho, A., Campos, D.A (Eds), *Tectonic Evolution of South America*. Rio de Janeiro, 297-310.

Valladares, C., Machado, N., Heilbron, M., Duarte, B., Gauthier, G., 2008. Sedimentary provenance in the central Ribeira belt based on laser-ablation ICPMS $^{207}Pb/^{206}Pb$ zircon ages. *Gondwana Research*, **13**, 4, 516-526.

Whitney, D.L., Evans, B.W., 2010. Abbreviations for names of rock-forming minerals. *American Mineralogist*, **95**, 185-187.

Wimmenauer, W., Bryhni, I., 2007. Migmatites and related rocks. In: Fettes, D., Desmons, J. (Eds), *Metamorphic Rocks: A Classification and Glossary of Terms*. IUGS, Cambridge University Press, New York, 43-45.